NACA RM E51J08

NACA

RESEARCH MEMORANDUM

PRELIMINARY INVESTIGATION OF USE OF CONICAL FLOW SEPARATION FOR EFFICIENT SUPERSONIC DIFFUSION

By W. E. Moeckel and P. J. Evans, Jr.

Lewis Flight Propulsion Laboratory
Cleveland, Ohio

NATIONAL ADVISORY COMMITTEE
FOR AERONAUTICS

WASHINGTON
December 17, 1951

NATIONAL ADVISORY COMMITTEE FOR AERONAUTICS

RESEARCH MEMORANDUM

PRELIMINARY INVESTIGATION OF USE OF CONICAL FLOW SEPARATION FOR EFFICIENT SUPERSONIC DIFFUSION

By W. E. Moeckel and P. J. Evans, Jr.

SUMMARY

The use of flow separation on a rod projecting upstream of a blunt body to decelerate the supersonic stream ahead of an annular nose inlet was investigated at Mach numbers of 1.76, 1.93, and 2.10. At each Mach number, the projection distance of the rod upstream of the nose was varied to determine the location for optimum diffusion efficiency. Maximum total-pressure recoveries were obtained with rod tip projections about 1.5 times the radius of the spherical nose and were higher than those obtained with single-shock solid cones. In the vicinity of the optimum tip projections, subcritical operation was similar to that observed with solid-cone inlets. The flow pattern upstream of the nose for supercritical operation was not appreciably affected by the high pressures downstream in the annular passage. The effect of angle of attack on the efficiency of the separation inlet was more severe than for solid-body inlets; a reduction in maximum total-pressure recovery from 90 to 81 percent was noted at a Mach number of 1.93 for an angle of attack of $4\frac{3}{4}^{\circ}$.

INTRODUCTION

In reference 1 it is pointed out that the presence of a boundary layer or wake upstream of an axially symmetric blunt body tends to produce a conical separated-flow region at supersonic speeds. This conical separation creates a flow field similar to that past a solid cone and should, consequently, be applicable for the compression of the supersonic stream ahead of an annular nose inlet. In the present report, results of an investigation of the operating characteristics of a separation-cone inlet are presented. The experiments were preliminary in the sense that no drag data were obtained and no attempts were made to improve the performance by means of internal contraction, boundary-layer control, or systematic variation of the location of the nose relative to the cowl. The investigation was conducted at the NACA Lewis laboratory.

DESCRIPTION OF MODEL

A sketch of the inlet used, with significant dimensions and notations, is shown in figure 1. The spherical-nosed center body with radius R = 0.375 inch and the projecting rods are the same as those used in the aerodynamics investigation reported in reference 2. All tests were run with a 1/4-inch strip of carborundum dust placed just downstream of the conical tip of the rods. In the investigation of reference 2, this strip produced a more nearly conical separation region at large tip projections than the rods without the carborundum strip. The annular passage between the center body and the cowl was designed to produce no internal contraction. Downstream of the portion of the inlet shown in figure 1, the body and the cowl were faired into, and attached to, the subsonic diffuser and simulated combustion chamber used in reference 3. A conical plug at the outlet of the combustion chamber was used to determine the variation of pressure recovery with mass flow through the diffuser.

The ratio of the distance of the nose upstream of the cowl l to the inlet radius of the cowl R_0 was initially selected so that the shock corresponding to a 50° conical separation, tangent to the nose, would pass just outside the lip at a free-stream Mach number of 2.0. During the course of the investigation, the nose was moved upstream 1/16-inch by means of a spacer between the nose and the afterbody. This modification was found to increase the total-pressure recovery considerably at a Mach number of 1.93. The internal lip angle (13°) is equal to the flow angle immediately downstream of the shock from a 50° cone at a Mach number of 2.0, but a wide range of local flow angles and Mach numbers could be tolerated without producing shock detachment.

As in references 2 and 3, the model was mounted on a flat plate and tested in the Lewis 18- by 18-inch tunnel. The test section Mach number and Reynolds number are 1.91 and 3.24×10^6 per foot, respectively. By altering the angle of attack of the flat plate, the model was tested at Mach numbers of 1.76, 1.93, and 2.10.

QUALITATIVE RESULTS

Schlieren photographs of the sequence of flow patterns obtained at a Mach number of 2.10 as the rod tip projection was progressively increased are shown in figure 2. These flow patterns correspond to the maximum pressure recovery attained at each tip projection. The ratio of the mean stagnation pressure in the combustion chamber to the free-stream stagnation pressure is P_c/P_0, and m_c/m_0 is the ratio of the mass flow through the inlet to the maximum possible mass flow. Mass flow through the combustion chamber was measured with a standard A.S.M.E. orifice plate and is accurate to within about ± 1 percent.

The flow patterns upstream of the cowl are identical with those obtained in reference 2 with no cowl. The transition from separation at the shoulder of the rod to separation on the downstream surface takes place, as in reference 2, for values of tip projection ratio R/L between 0.3 and 0.25 (figs. 2(f) and 2(g)). The second oblique shock with origin near the point of contact of the separation boundary and the solid nose was noted also in reference 2 and appeared to be unaffected by the presence of the cowl at peak pressure recovery. The flow patterns corresponding to peak pressure recovery (fig. 2) were not noticeably changed as the outlet area was increased, although some increase in mass flow was obtained.

In figures 2(a) and 2(b) a detached shock can be seen at the cowl lip. This shock is a result of the relatively large flow deflection angles and the relatively low Mach number just downstream of the second oblique shock. As the tip projection is increased, the second shock becomes weaker; and, for $R/L < 0.5$, an attached shock appears at the lip. The maximum pressure recovery and mass flow, however, decrease between $R/L = 0.7$ and $R/L = 0.3$. When the separation shifts from the tip to the rod surface (fig. 2(f) and 2(g)), the pressure recovery and mass flow again increase but reach a maximum lower than the first (fig. 2(i)).

The first maximum in pressure recovery and mass flow occurs when the half-angle of the conical separation region is about 25° (fig. 2(b)). The peak recoveries at Mach numbers of 1.76 and 1.93 also occurred near the tip projections corresponding to this angle. This result corresponds closely with that obtained with solid cones in reference 4, where both analytical and experimental peak pressure recoveries were obtained with 25° half-angle cones.

The chief differences between flow patterns obtained at a Mach number of 2.10 and those obtained at Mach numbers of 1.76 and 1.93 can be seen in figure 3, where the configurations corresponding to the maximum value of P_c/P_0 attained at each Mach number are shown. At a Mach number of 1.76 (fig. 3(a)), the detached wave at the lip of the cowl extends farther upstream and appears to have absorbed the second oblique shock observed at the higher Mach numbers. The higher deflection angle and lower Mach number near the lip at a Mach number of 1.76 account in part for the difference in flow pattern. Another reason for the difference is the smaller nose projection distance l used at Mach number 1.76. The tests at a Mach number of 1.76 were run first, with the ratio $l/R_0 = 0.25$. At a Mach number of 1.93 it was found that higher pressure recoveries were attained when l was increased 1/16-inch, corresponding to a value of l/R_0 of 0.35. A further increase in l to a distance 1/8-inch upstream of the original position

yielded lower pressure recoveries than the 1/16-inch increase. Consequently, all subsequent tests at Mach numbers of 1.93 and 2.10 were run with $l/R_0 = 0.35$. It appears likely that the pressure recovery at a Mach number of 1.76 would also have been somewhat higher with a larger nose projection and that the second oblique shock would have appeared. At each Mach number, a redesign of the inlet lip to correspond to the flow angle behind the second oblique shock should raise the mass flow by eliminating the detached shock at the lip of the cowl.

The effect of angle of attack on the flow pattern at a Mach number of 1.93 is shown in figure 4, where the configuration which yielded the highest efficiency at zero degrees (fig. 3(b)) is inclined at an angle of attack of 4.75°. The pressure recovery is reduced about 12 percent at this angle of attack. The reason for the large reduction is evident from the Schlieren photograph; a strong shock wave is seen near the lower surface of the spherical nose. The separated-flow region evidently does not support the pressure difference between top and bottom surfaces of a solid cone at angle of attack but tends, instead, to aline itself with the stream direction to minimize the pressure differential. A larger flow deflection results at the bottom surface of the nose, and the consequent strong shock reduces the pressure recovery.

The subcritical operation of the separation inlet was found to be of the same nature as solid-body inlets, in that pulsing was observed for a mass-flow ratio below that corresponding to peak pressure recovery. For mass-flow ratios only slightly less than the peak recovery values, pulses were infrequent and random in time. As the mass flow was progressively reduced, pulses became more frequent and the interval between pulses more nearly constant. One of the pulses obtained at a fairly low mass-flow ratio is shown in figure 5, together with the predominant steady flow pattern. A series of eight flash photographs were taken, of which only one showed the pulse (fig. 5(b)). Methods used to reduce or eliminate subcritical pulsing with solid-body inlets should be equally effective with the separation inlet, since the instability appears to be in no way related to the presence of the separated flow region.

QUANTITATIVE RESULTS

In figures 6(a), 7(a), and 8(a) are shown the variations with tip projection of maximum total-pressure recovery and the corresponding mass flows at each of the Mach numbers investigated. The variation of total-pressure recovery with mass flow at the optimum tip projections are shown in figures 6(b), 7(b), and 8(b).

At a Mach number of 1.76 (fig. 6) the effect on inlet characteristics of changing the rod radius from 0.17 R to 0.25 R is shown. The thicker rod yielded somewhat higher pressure recoveries at small tip projections (large R/L); consequently, this rod was used in all subsequent tests at the higher Mach numbers. At small values of R/L, however, for which separation occurs on the surface of the rod, higher pressure recoveries were obtained with the thinner rod. This result is understandable from the consideration that a conical deflection produces a more efficient deceleration than a two-dimensional compression, and a thin rod produces a more nearly conical flow than a thick rod. The reason for the higher pressure recovery produced by the thicker rod under the tip-separation condition is not so evident since the shock patterns for the peak pressure recovery condition were almost identical for the two rod radii (compare figs. 3(a) and 5(a)).

The effect of angle of attack α on the maximum pressure recovery and mass flow is shown for a Mach number of 1.93 in figure 7. The difference between the maximum recovery at $\alpha = 0$ and at $\alpha = 4.75^{\circ}$ becomes greater as R/L is decreased from 1.0. A maximum difference is reached when the location of separation changes from the tip to the rod surface. In general, it appears that the effect of angle of attack on pressure recovery becomes greater as the separation-cone angles become smaller. The maximum pressure recoveries at an angle of attack of 4.75° were obtained with the smallest tip projections investigated and were about 10 percent lower than the maximum pressure recovery attained at zero angle of attack.

The form of the maximum pressure recovery curves as a function of tip projection ratio R/L at zero angle of attack corresponds closely, at each Mach number, to the form of the drag coefficient curves obtained in reference 2, except that, for large R/L, the drag continued to increase, whereas the pressure recovery reaches a maximum at $R/L \approx 0.70$. Both drag and pressure recovery reach a minimum when transition from separation at the tip to separation on the rod surface occurs. For tip projections greater than the critical value, both pressure recovery and drag increase to a maximum and then begin a gradual decrease as the tip projection becomes very large.

As shown in figures 6(b), 7(b), and 8(b), a gradual increase in mass-flow ratio was obtained as the outlet area of the diffuser was increased beyond the value corresponding to maximum pressure recovery. A possible explanation for this increase may be as follows: In reference 2 it is suggested that the entrainment of air by the main stream as it passes over the separated region may produce a reversed flow near the point of contact of the separated region with the solid nose. This reversed flow, which may be responsible for the second oblique shock, could be influenced by the back pressure and might be expected to

decrease in magnitude as the back pressure is decreased. This tentative explanation suggests that somewhat higher mass-flow ratios could be obtained by locating the internal normal shock sufficiently far downstream so that its effect on the separated region would be negligible even at peak pressure recovery. A relatively long constant-area passage may, therefore, be beneficial for the separation-type inlet.

COMPARISON WITH OTHER INLETS

In figure 9, the maximum pressure recoveries and corresponding mass-flow ratios obtained with the separation inlet are compared with the values obtained in reference 3 for several types of solid-body inlet and with a theoretical curve for the maximum pressure recovery obtainable with a 50° cone followed by a normal shock is included. Although the inlets of reference 3 were not optimum configurations, they can be considered as roughly equivalent in development stage to the separation inlet investigated herein. Higher mass flows (and consequently lower additive drags) were obtained with the inlets reported in references 5 and 6, but the pressure recoveries were considerably lower than those reported in reference 3. Since no attempt was made to maximize the mass flow for the separation inlet (by redesigning the cowl lip), the comparison with results of reference 3 is believed to be reasonably valid.

The pressure recoveries attained with the separation inlet at Mach numbers of 1.93 and 2.10 are higher than those obtained with a solid 50° cone and are only about 2 percent lower than the maximum theoretical values for a single-shock cone inlet. Since the losses in the subsonic portion of the diffuser are probably greater than 2 percent, it is evident that the second oblique shock contributed materially to the pressure recovery of the separation inlet. This inlet should therefore be classed as a double oblique shock inlet, and pressure recoveries corresponding to such an inlet should be attainable. The data of figure 9 show that in these preliminary tests the separation inlet is intermediate between the single-shock inlet and the isentropic center-body inlet both with regard to maximum pressure recovery and corresponding mass flow at Mach numbers of 1.93 and 2.10. At a Mach number of 1.76, where no attempt was made to raise the maximum pressure recovery by changing the body projection l, the maximum pressure recovery is below the solid-cone value; but the mass flow is considerably higher.

Except for the large effect of angle of attack, the separation inlet appears to have no serious disadvantages relative to solid-body inlets. The strong effect of angle of attack could probably be reduced by providing a splitter plate to isolate the upper and lower portions of the separated region. Such a modification, however, might reduce

the effectiveness of the separation inlet at subsonic speeds and for radome application. Other possibilities are to rotate the spherical nose so that alinement of the rod with the free-stream direction is preserved or to provide a feedback tube between the combustion chamber and the nose to regulate the pressure in the separated region and, consequently, the effective cone angle of the compression surface. Some research on alleviation of angle of attack effects appears necessary before the separation inlet can be considered operationally equal to the solid-body inlet.

CONCLUDING REMARKS

The use of flow separation on a rod projecting upstream of a blunt body to decelerate a supersonic stream was investigated at Mach numbers of 1.76, 1.93, and 2.10. Pressure recoveries and mass-flow ratios comparable with those obtained with solid-center-body inlets were obtained. Subcritical instability was found to be of the same nature as that obtained with solid-body inlets. The effect of angle of attack in reducing the efficiency of the inlet was more severe than for solid-body inlets, because of the tendency of the separation cone to aline itself with the free-stream direction. Research to reduce the strong angle of attack effect may be necessary before the separation inlet can be considered equivalent to a solid-body inlet from the operational standpoint.

Lewis Flight Propulsion Laboratory
National Advisory Committee for Aeronautics
Cleveland, Ohio

REFERENCES

1. Moeckel, W. E.: Flow Separation Ahead of Blunt Bodies at Supersonic Speeds. NACA TN 2418, 1951.

2. Moeckel, W. E.: Flow Separation Ahead of a Blunt Axially-Symmetric Body at Mach Numbers 1.76 to 2.10. NACA RM E51I25, 1951.

3. Fox, Jerome L.: Supersonic Tunnel Investigation by Means of Inclined-Plate Technique to Determine Performance of Several Nose Inlets over Mach Number Range of 1.72 to 2.18. NACA RM E50K14, 1951.

4. Moeckel, W. E., Connors, J. F., and Schroeder, A. H.: Investigation of Shock Diffusers at Mach Number 1.85. I - Projecting Single-Shock Cones. NACA RM E6K27, 1947.

5. Obery, L. J., and Englert, G. W.: Force and Pressure Characteristics for a Series of Nose Inlets at Mach Numbers from 1.59 to 1.99. II - Isentropic-Spike All-External Compression Inlet. NACA RM E50J26a, 1951.

6. Weinstein, Maynard I., and Davids, Joseph: Force and Pressure Characteristics for a Series of Nose Inlets at Mach Numbers from 1.59 to 1.99. III - Conical-Spike All-External-Compression Inlet with Supersonic Cowl Lip. NACA RM E50J30, 1951.

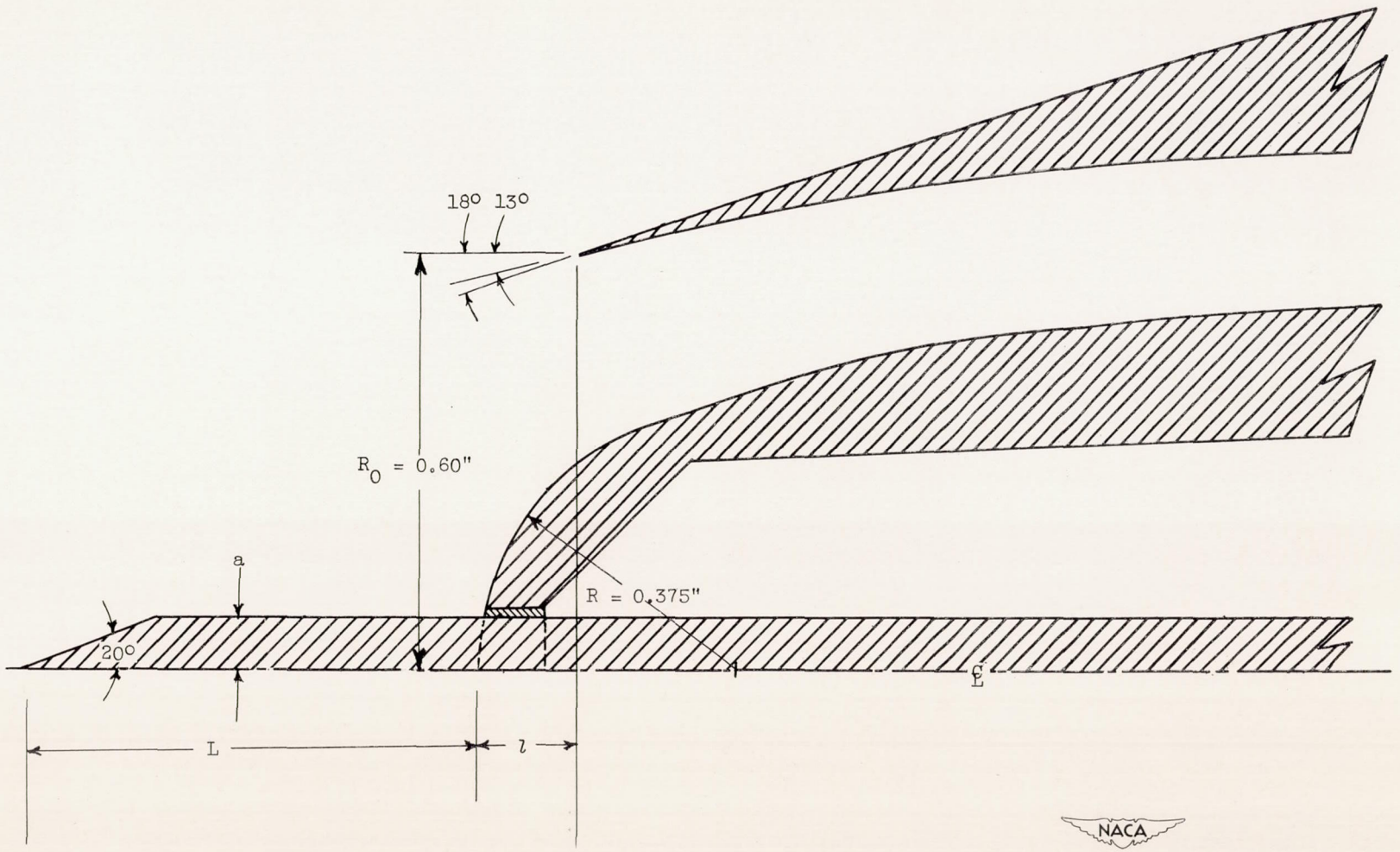

Figure 1. - Significant dimensions and notation for separation inlet model.

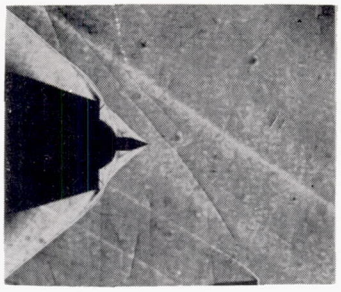

(a) $\frac{R}{L} = 0.826$;
$\frac{P_c}{P_0} = 0.838$;
$\frac{m_c}{m_0} = 0.845$.

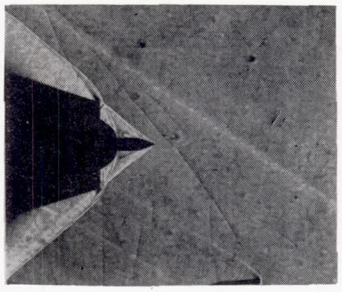

(b) $\frac{R}{L} = 0.698$;
$\frac{P_c}{P_0} = 0.853$;
$\frac{m_c}{m_0} = 0.866$.

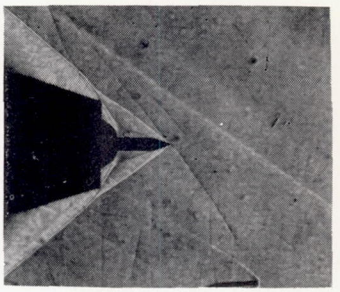

(c) $\frac{R}{L} = 0.500$;
$\frac{P_c}{P_0} = 0.807$;
$\frac{m_c}{m_0} = 0.841$.

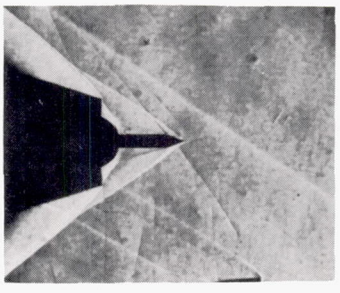

(d) $\frac{R}{L} = 0.402$;
$\frac{P_c}{P_0} = 0.755$;
$\frac{m_c}{m_0} = 0.814$.

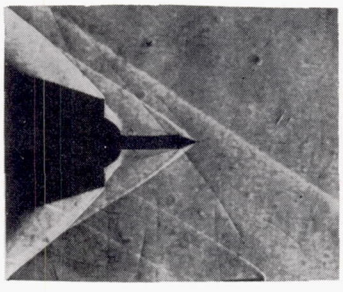

(e) $\frac{R}{L} = 0.350$;
$\frac{P_c}{P_0} = 0.734$;
$\frac{m_c}{m_0} = 0.789$.

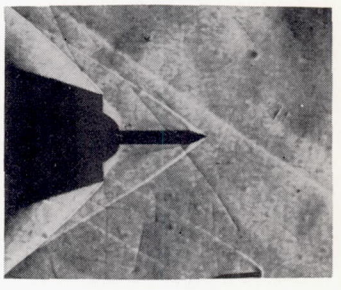

(f) $\frac{R}{L} = 0.300$;
$\frac{P_c}{P_0} = 0.705$;
$\frac{m_c}{m_0} = 0.768$.

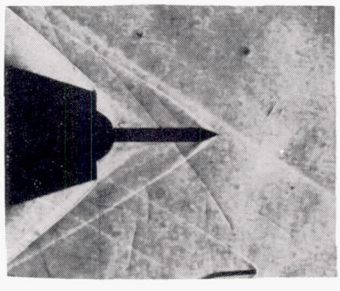

(g) $\frac{R}{L} = 0.249$;
$\frac{P_c}{P_0} = 0.749$;
$\frac{m_c}{m_0} = 0.840$.

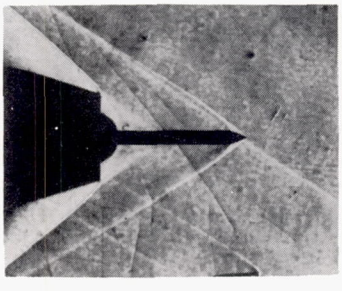

(h) $\frac{R}{L} = 0.201$;
$\frac{P_c}{P_0} = 0.751$;
$\frac{m_c}{m_0} = 0.835$.

NACA
C-28347

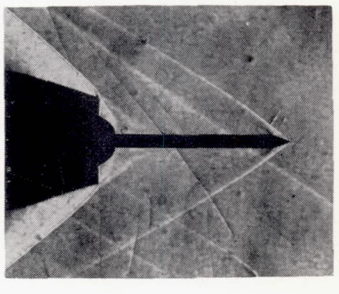

(i) $\frac{R}{L} = 0.150$;
$\frac{P_c}{P_0} = 0.752$;
$\frac{m_c}{m_0} = 0.836$.

Figure 2. - Flow patterns corresponding to peak pressure recovery for several tip projections. $M_0 = 2.10$; $\frac{a}{R} = 0.25$; $\alpha = 0^\circ$; $\frac{l}{R_0} = 0.35$.

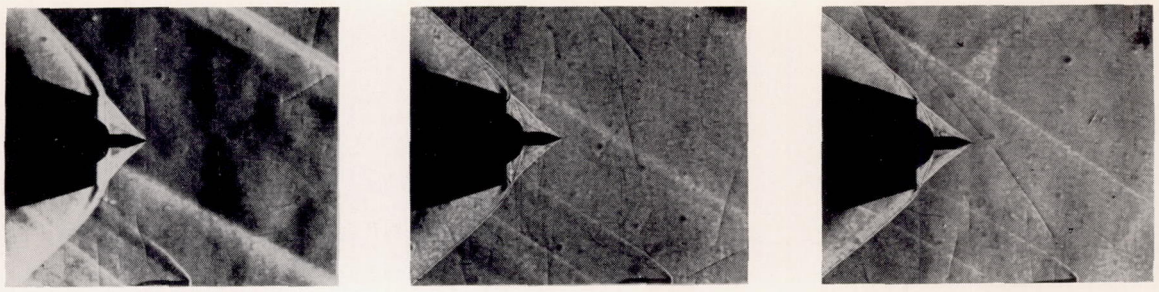

(a) $M_0 = 1.76$; $\frac{R}{L} = 0.688$; $\frac{l}{R_0} = 0.25$; $\frac{P_c}{P_0} = 0.906$; $\frac{m_c}{m_0} = 0.824$.

(b) $M_0 = 1.93$; $\frac{R}{L} = 0.702$; $\frac{l}{R_0} = 0.35$; $\frac{P_c}{P_0} = 0.902$; $\frac{m_c}{m_0} = 0.805$.

(c) $M_0 = 2.10$; $\frac{R}{L} = 0.698$; $\frac{l}{R_0} = 0.35$; $\frac{P_c}{P_0} = 0.853$; $\frac{m_c}{m_0} = 0.865$.

NACA
C-28359

Figure 3. - Flow patterns corresponding to highest pressure recovery attained at each Mach number. $\frac{a}{R} = 0.25$.

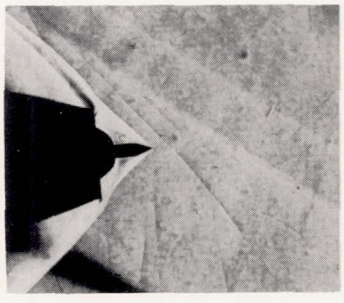

NACA
C-28360

Figure 4. - Effect of angle of attack on flow pattern. $M_0 = 1.93$; $\frac{a}{R} = 0.25$; $\frac{l}{R_0} = 0.35$; $\alpha = 4.75^\circ$; $\frac{R}{L} = 0.698$; $\frac{P_c}{P_0} = 0.784$; $\frac{m_c}{m_0} = 0.790$.

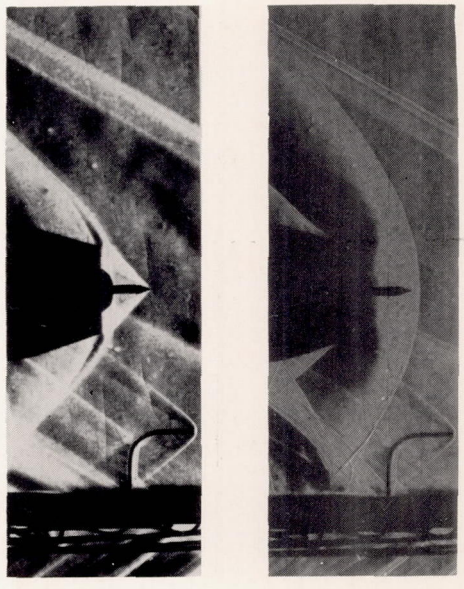

(a) Regular exposure. (b) Flash exposure.

NACA
C-28346

Figure 5. - Illustration of subcritical pulse. $M_0 = 1.76$; $\frac{a}{R} = 0.17$; $\frac{R}{L} = 0.694$; $\frac{m_c}{m_0} = 0.612$; $\frac{l}{R_0} = 0.25$; $\frac{P_c}{P_0} = 0.853$.

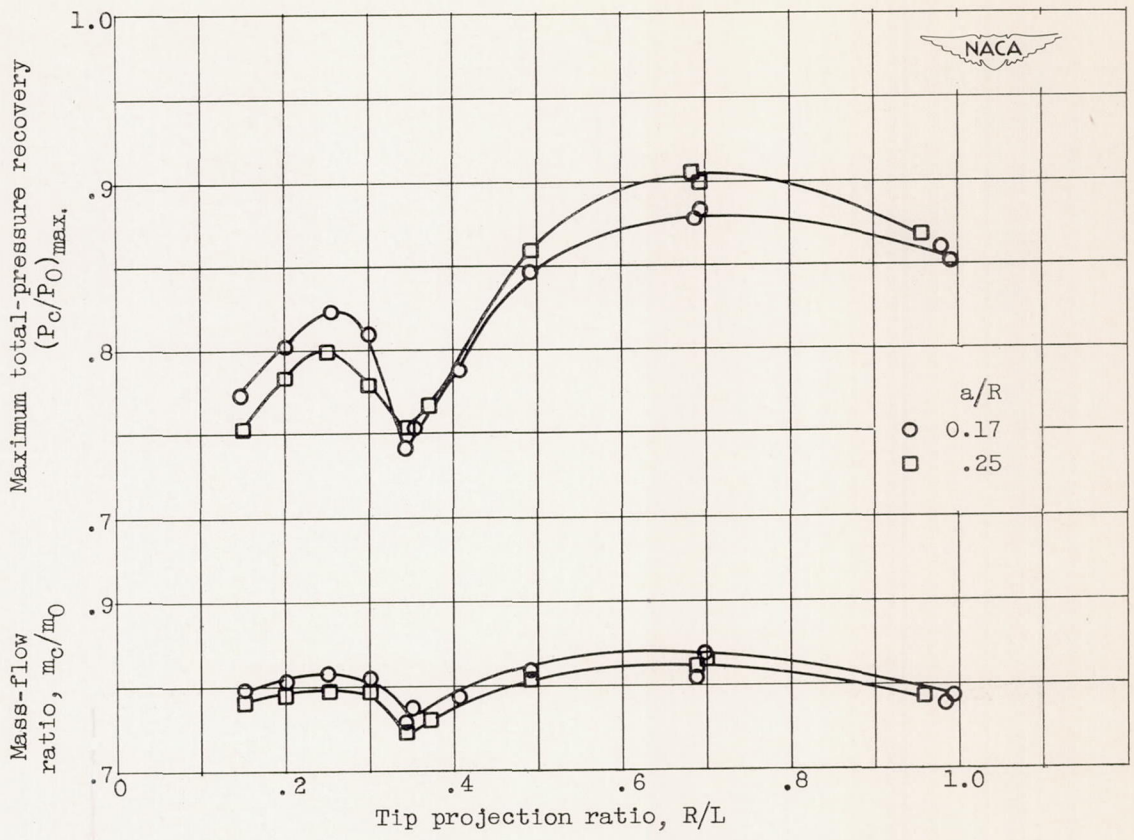

(a) Maximum total-pressure recovery and corresponding mass-flow ratio as function of tip projection.

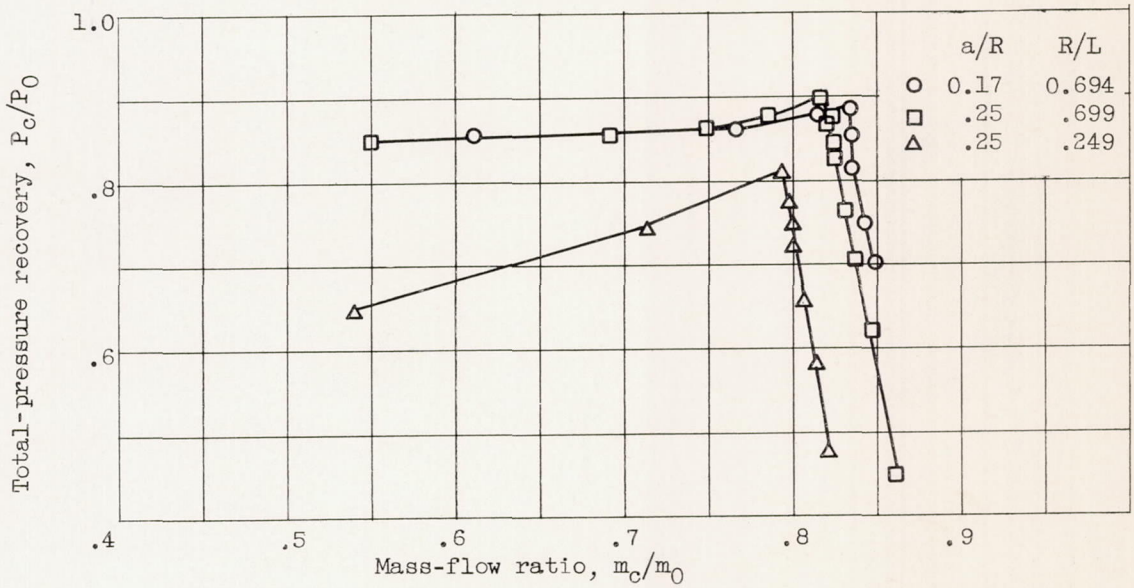

(b) Mass flow - pressure recovery relations at optimum R/L.

Figure 6. - Inlet characteristics for Mach number of 1.76.

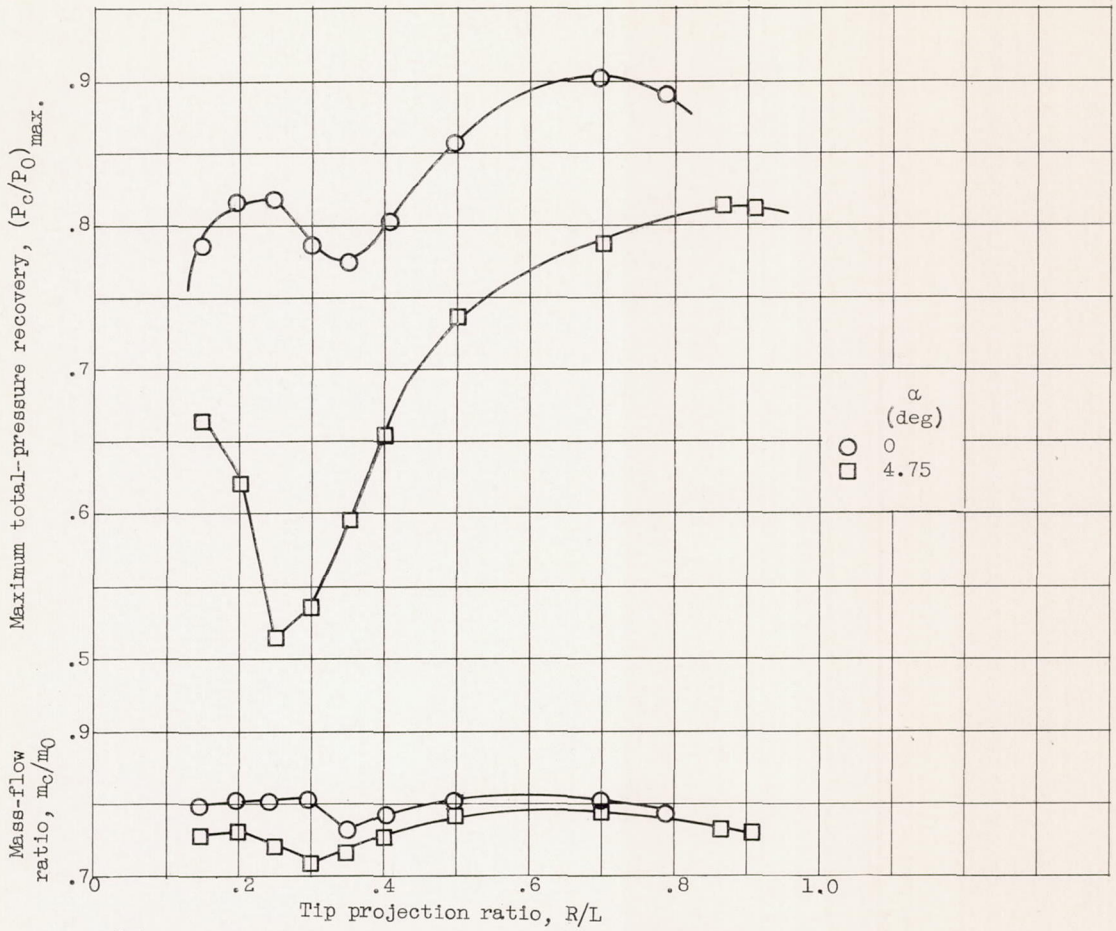

(a) Maximum total-pressure recovery and corresponding mass-flow ratio as function of tip projection.

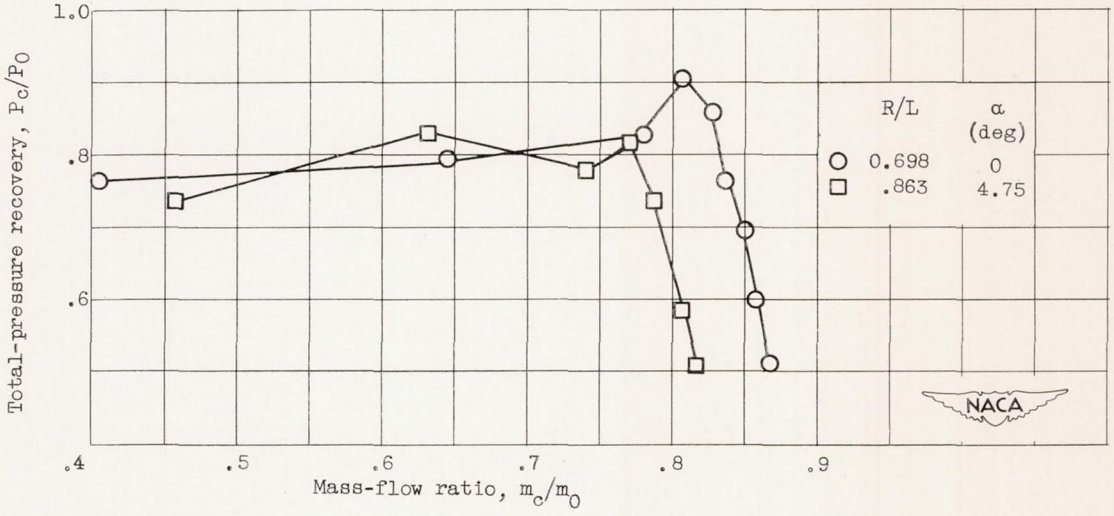

(b) Mass flow - pressure recovery relation at optimum R/L.

Figure 7. - Inlet characteristics at Mach number of 1.93. a/R = 0.25.

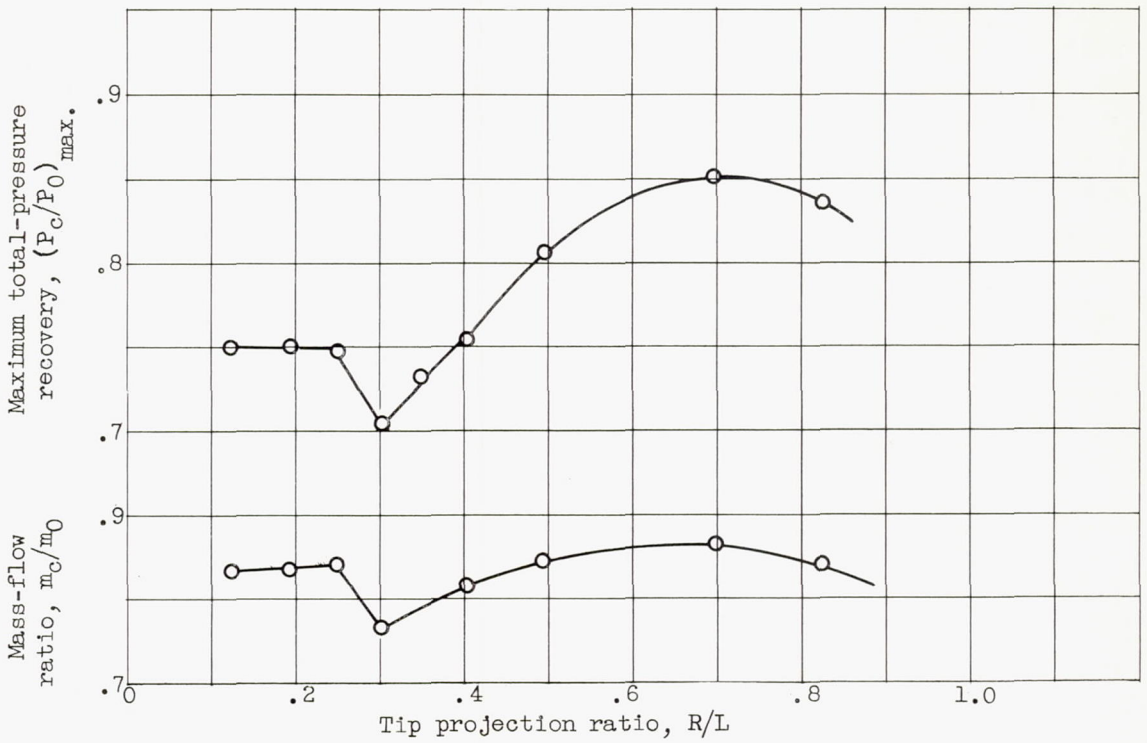

(a) Maximum total-pressure recovery and corresponding mass-flow ratio as function of tip projection.

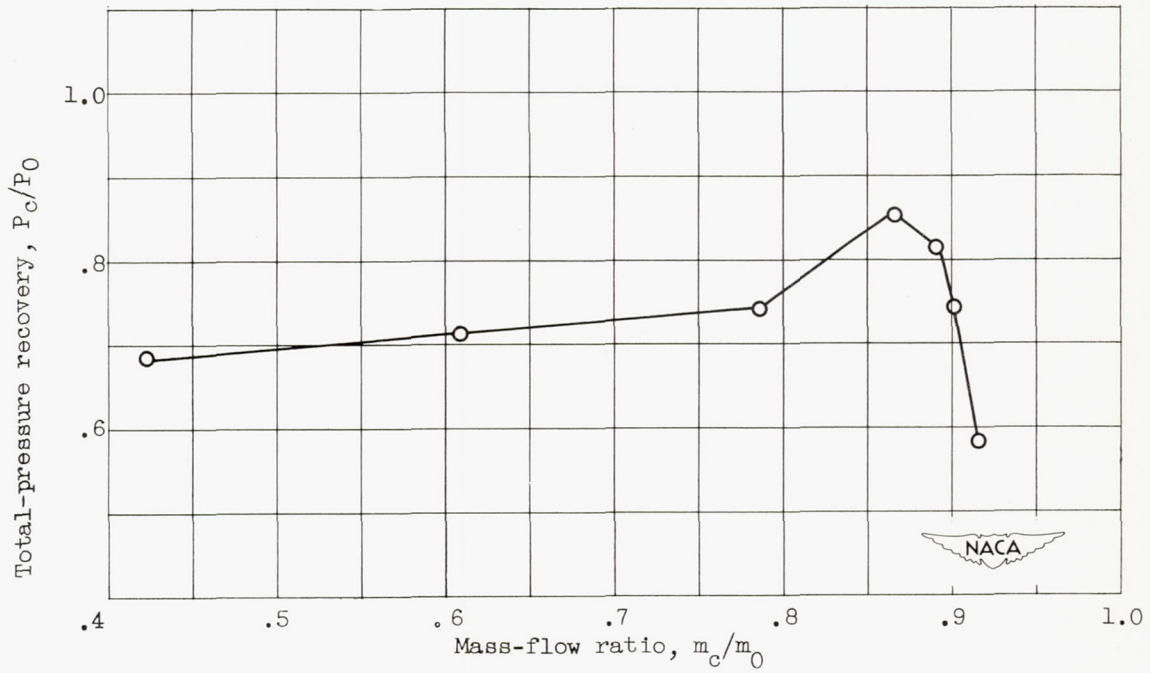

(b) Mass flow - pressure recovery relation at optimum R/L (0.698).

Figure 8. - Inlet characteristics for M_0 = 2.10. a/R = 0.25; $\alpha = 0^\circ$.

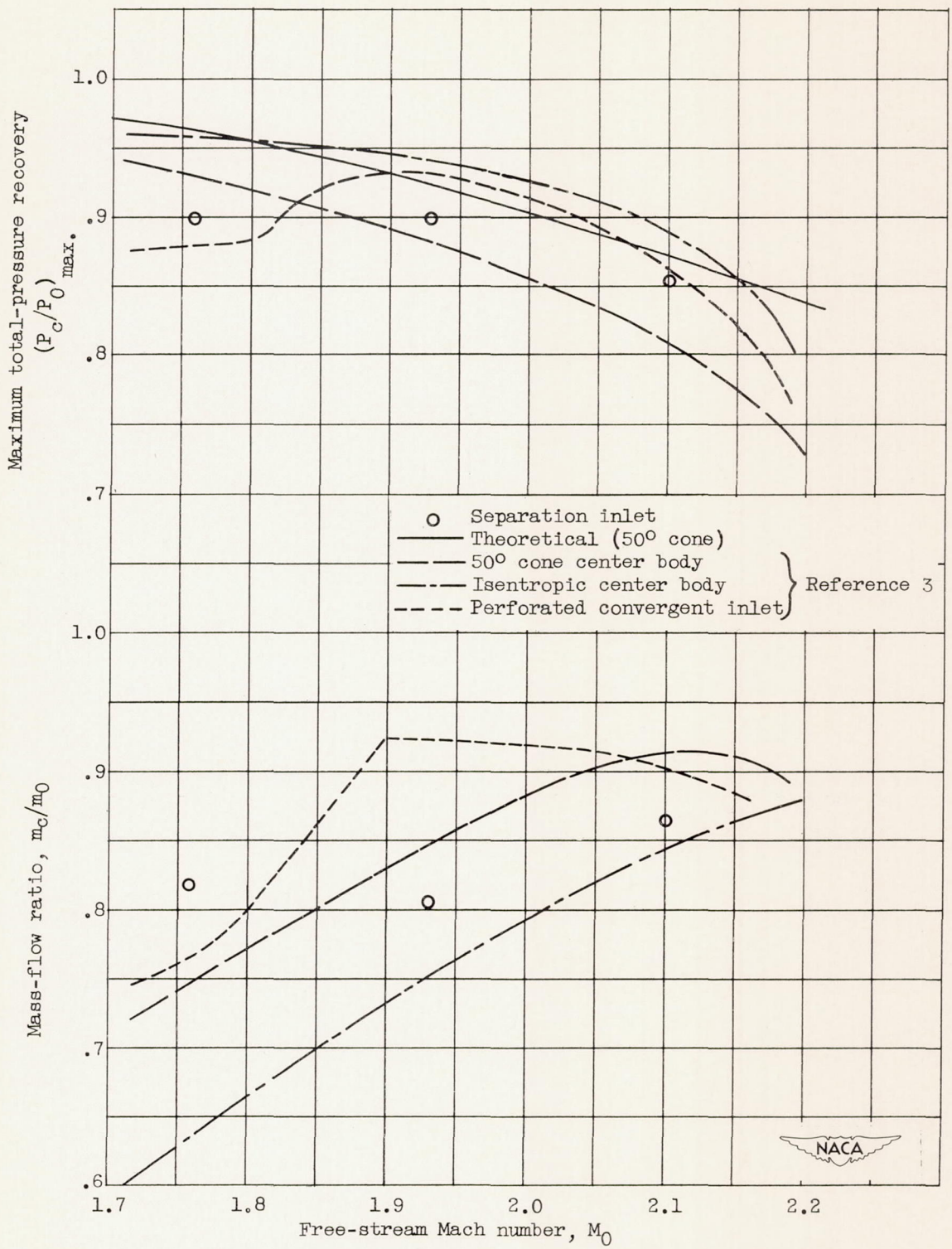

Figure 9. - Maximum total-pressure recovery and corresponding mass-flow ratio for separation inlet and several solid-body inlets.